LETTERS
PUBLISHED ONLINE: 30 OCTOBER 2011 | DOI: 10.1038/NGEO1309
nature geoscience

Tibetan plate overriding the Asian plate in central and northern Tibet

Wenjin Zhao[1], Prakash Kumar[2,3], James Mechie[2], Rainer Kind[2,4]*, Rolf Meissner[5], Zhenhan Wu[1], Danian Shi[1], Heping Su[1], Guangqi Xue[1], Marianne Karplus[6] and Frederik Tilmann[2,4]

The southern boundary between India and the Tibetan Plateau represents a classical case of continental subduction, where the Indian continental lithosphere is subducted northwards beneath the Tibetan Plateau[1–6]. At the northern boundary, southward subduction of Asian lithosphere beneath the Tibetan Plateau has also been proposed[7], but imaging has been hampered by inadequate data quality. Here we analyse the plate tectonic structure of the northern boundary between Tibet and Asia using the S receiver function technique. Our passive source seismic data build on, and extend further northwards, the existing geophysical data from the International Deep Profiling of Tibet and the Himalaya project[8–10]. We detect, beneath central and northern Tibet, a relatively thin, but separate, Tibetan lithosphere overriding the flat, southward subducting Asian lithosphere. We suggest that this overriding Tibetan lithosphere helps to accommodate the convergence between India and Asia in central and northern Tibet. We conclude that the Tibetan–Himalayan system is composed of three major parts: the Indian, Asian and Tibetan lithospheres. In the south, the Indian lithosphere underthrusts Tibet. In central and northern Tibet a separate, thin Tibetan lithosphere exists, which is underthrust by the Asian lithosphere from the north.

In the seismic experiment discussed here (International Deep Profiling of Tibet and the Himalaya (INDEPTH) IV; ref. 11, see inset in Fig. 1 for location), 32 German and 24 British seismic stations have been operated from early summer 2007 until late summer 2008 in two dense linear profiles. The station spacing across two suture zones was only about 4 km. The receiver function method, which is applied for processing the seismic data, is especially useful to image seismic discontinuities in the lithosphere. It is a well established method and has been applied to Tibetan data in previous studies (for example, refs 2,12,13). It uses waves converted (S-to-P or P-to-S in the S- or P- receiver function technique, respectively) at seismic discontinuities (for example, crust–mantle boundary–Moho; or lithosphere–asthenosphere boundary (LAB)) for detecting these discontinuities and describing their properties. The S receiver function technique is especially useful for studies of upper mantle discontinuities, mainly the LAB, because the multiply reflected phases do not interfere with the direct converted phases. Multiple reflections are sometimes a problem in P receiver functions.

Figure 2b shows P receiver function data along the INDEPTH line (INDEPTH projects II, III and IV), the 1991/92 Sino-US PASSCAL experiment[14], data of the permanent station at Lhasa and from some earlier projects (see Supplementary Information for location of all stations used). The global reference model IASP91 was used for the migration of seismograms from the time to depth domain. The Moho is clearly visible along the entire profile (black dashed line, marked '1'). A south dipping converter (a discontinuity in material properties which converts seismic waves), already seen in earlier work[2], is also visible (black dashed line, marked '2'). We interpreted this discontinuity as the Moho of the subducting Asian crust[2]. The coloured thick dashed lines (in red, blue and green) are LAB observations from S receiver functions taken from Fig. 2d. The deeper part of the signal, marked '2', seems to cut the Asian LAB (marked green). However, the first Moho multiple interferes with the signal from the '2' discontinuity below ~160 km, such that this effect is probably an artefact. The receiver functions of INDEPTH IV alone do not show this effect (see Supplementary Fig. S6).

Figure 2c shows details of the INDEPTH IV data across the Kunlun fault (KF) system. The Moho shallows from about 70 to 50 km within about 100 km towards the north, confirming other

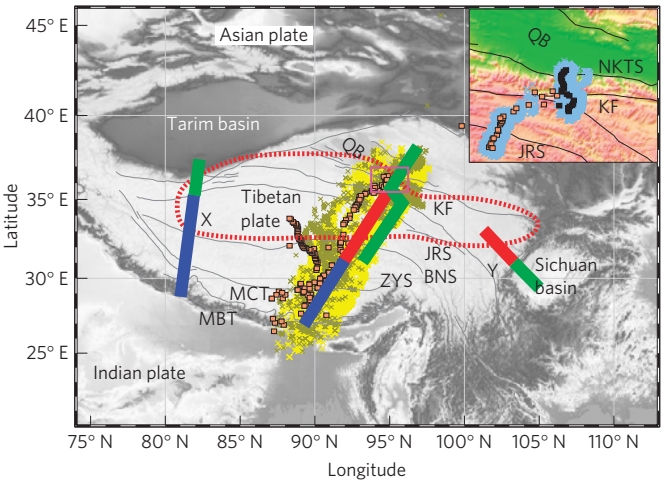

Figure 1 | Topographic map and location of seismic profiles. Squares are seismic stations (INDEPTH IV in inset). Yellow region is sampled at 410 km depth; area with crosses at 120 km, blue area in inset at 70 km. Coloured bars indicate LAB observations: blue = India, green = Asia, red = Tibet. Region within red dashed line shows high attenuation of seismic waves[8,9]. X and Y mark profiles towards the Tarim and Sichuan basins[1,6]. MBT=Main Boundary Thrust, MCT = Main Central Thrust, BNS = Banggong Nujiang Suture, JRS = Jinsha River Suture, NKTS = North Kunlun Thrust System, QB = Qaidam basin.

[1]Chinese Academy of Geological Sciences, Beijing 100037, China, [2]Deutsches GeoForschungsZentrum GFZ, Potsdam 14473, Germany, [3]National Geophysical Research Institute (CSIR), Hyderabad 500037, India, [4]Freie Universität Berlin, Institut für Geologische Wissenschaften, Berlin 12249, Germany, [5]Universität Kiel, Institut für Geowissenschaften, Kiel 24118, Germany, [6]Stanford University, Stanford, California 94305, USA.
*e-mail: kind@gfz-potsdam.de.

© 2011 Macmillan Publishers Limited. All rights reserved.

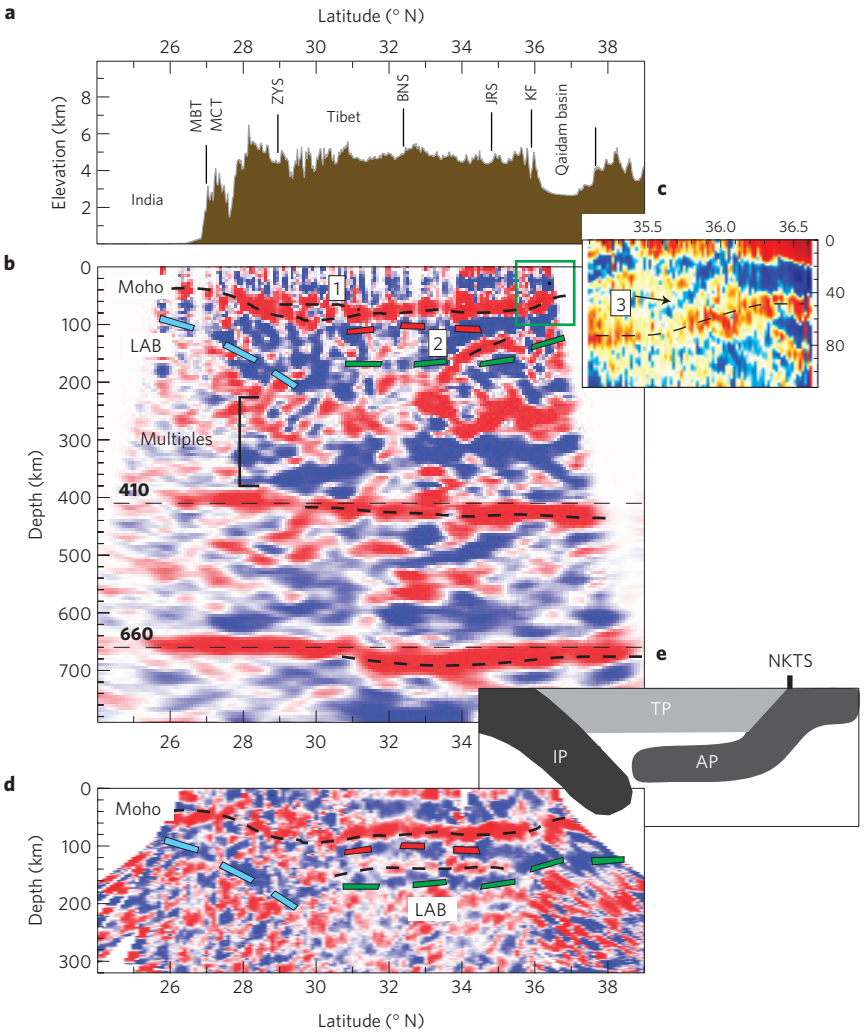

Figure 2 | Receiver function data along the INDEPTH profiles. a, Topography **b**, P receiver functions. 1 = Moho 'doublet', 2 = Asian Moho, 410, 660 = discontinuities at these depths (theoretical location = longer dashes). Coloured dashed lines copied from **d**. **c**, Zoom across KF (black squares in Fig. 1 inset). 3 = dipping structure within the crust (Supplementary Information). **d**, S receiver functions. Moho = black dashed line; lower black dash line = weak indication of Moho of Asian lithosphere. Blue, red and green dashed lines = LAB of Indian, Tibetan and Asian plates, respectively. Same data without marked features can be seen in Supplementary Fig. S1. **e**, Cartoon of resulting model. IP = Indian, TP = Tibetan, AP = Asian plates, respectively; NKTS = North Kunlun Thrust System[25] (Supplementary Information).

results (refs 15–18). Indications of Tibetan lower crust indenting across the KF system into the Qaidam crust[18,19] are not observed in our data owing to their relatively long periods. We also see no direct connection between the Qaidam Moho and signal '2' in Fig. 2b, which was interpreted as subducting Asian Moho. This might be due to a true gap in the subducting crust or an effect of the interference of relatively long-period seismic signals. A negative (blue, meaning velocity decrease downwards) inclined structure within the crust is also observed (marked '3' in Fig. 2c). This can be interpreted as low-velocity Qaidam crustal material underthrusting higher-velocity northern Tibetan crust. No comparable structure is seen in receiver function data at the boundary between the Indian and Tibetan crusts, the Zangbo-Yarlung Suture (ZYS). A much more complicated structure was found there—the so-called 'Moho doublet'[20–22], which was interpreted as being caused by Indian lower crust not participating in the subduction of the mantle lithosphere but continuing to the north at a deep crustal level. The Moho structure thus exhibits three different regimes along the INDEPTH profiles across Tibet. South of the ZYS we see an increase of the Moho depth from about 40 km in India to about 80 km in Tibet. From the ZYS to the KF system we see a relatively homogeneous but slightly shallowing Moho. The Banggong Nujiang Suture and the Jinsha River Suture do not significantly influence the Moho depth. At the KF system we see a rapid Moho shallowing from about 70 km–50 km in the Qaidam basin.

Figure 2d shows S receiver function data along the INDEPTH line. The Moho (marked red) is clearly visible and confirms the corresponding P receiver function observations. Negative (blue) signals are observed above and below the Moho. They indicate velocity reductions downwards. Crustal low-velocity zones have been observed previously (for example, refs 2,20). Mainly based on the recent INDEPTH IV data is the new observation of a negative structure between the Moho and the Asian LAB (green dashed line) in central and northern Tibet at 100–120 km depth (marked by a red dashed line in Fig. 2d). This phase is interpreted as the LAB of the Tibetan terranes. It is relatively close to the Moho signal; therefore side-lobe problems should be discussed. In the Supplementary Information we have done this. Side-lobe signals should, with increasing periods, move further away from the main signal. We have filtered our data with different main periods and found the LAB signal remaining stable at the same time. This makes us very confident that the observed Tibetan LAB is a real signal

© 2011 Macmillan Publishers Limited. All rights reserved.

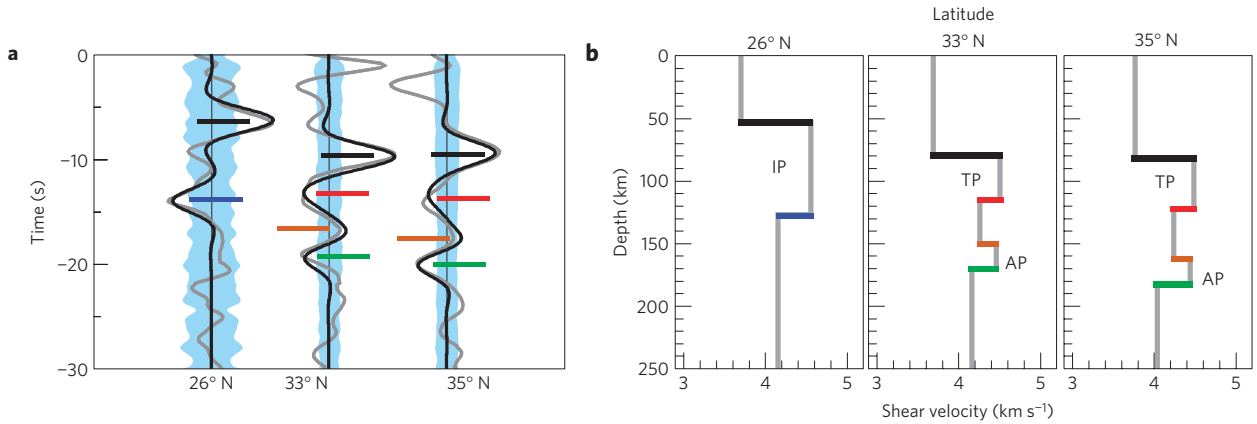

Figure 3 | Waveform forward modelling. a, Waveform comparison of observed and theoretical S receiver functions; grey = observed, black = theoretical. Blue area marks the ±2 standard error. **b**, Models used for computation of theoretical seismograms. Coloured bars: blue = Indian, green = Asian and red = Tibetan LABs, respectively (colours as in Fig. 2); black = Tibetan Moho, brown = weak Asian Moho (see Fig. 2d). Velocity jump at the Moho resulting from amplitude fitting is ~17.7 ± 2.5% in all models. The contrast across the Indian LAB is 9.1 ± 2.2%, across the Tibetan LAB is 5.5 ± 1.3% and across the Asian LAB it ranges between 6.7 and 8.9 ± 1.5%. The ±2 standard error in time is estimated to be 0.5 s. All errors are obtained using bootstrapping. The resulting depth error of the LAB is about ±5 km.

and not a side lobe. It is visible over a distance of 400–500 km. As the Moho is located at 70–90 km depth, the mantle lithosphere of the Tibetan plate has a thickness of only ~30 km. The Tibetan LAB is only observed south of the KF system, where the Asian LAB suddenly deepens (see Supplementary Fig. S2, for further images in the time domain). The Indian LAB (blue dashed line) and parts of the Asian LAB (green dashed line) have been observed previously[2]. Subduction of the Qaidam basin below northern Tibet has already been suggested on the basis of crustal shortening and northeastward propagation of south-dipping thrust fault systems at the northern edge of Tibet[7,23,24]. Here we clearly image this subduction with seismic data (green dashed line in Fig. 2d).

Similar to the appearance of the Moho across Tibet, we also observe three regimes in the LAB structure. In the south we see the subducting Indian LAB reaching just to the north of the ZYS. Between the ZYS and KF system we see two LABs, which we interpret as a surprisingly homogeneous Tibetan LAB overriding the Asian LAB. North of the KF system we see a normal cratonic LAB, similar to the Indian LAB. Unfortunately our data do not reach very far north of the KF system.

Northern Tibet with the Tibetan lithosphere stacked on top of the Asian lithosphere is also a region where Sn (travelling in the mantle lid) does not propagate effectively and Pn (travelling also in the mantle lid) has a low velocity[25–27] (see marked region in Fig. 1). These observations indicate that the Tibetan lithosphere in this area may also have a higher temperature than, for example, the subducting Indian lithosphere further south. Low average velocities in the upper mantle in the northern part of the profile are also indicated by about 20 km (5%) deepened signals from both discontinuities at 410 and 660 km depth (Fig. 2b).

Figure 3a shows a comparison of observed and computed S receiver functions at three locations along the INDEPTH line. The velocity–depth models used are shown in Fig. 3b. Average crustal velocity is taken from ref. 10 and the V_p/V_s ratios from ref. 20. Velocity ratios at the Moho and LAB were obtained from fitting the Moho and LAB amplitudes. The velocity in the asthenosphere seems low below the Asian and Indian LAB, but they could be confined to the vicinity of the LAB. The velocity in the thin piece of asthenosphere below the Tibetan LAB seems more normal. This could be a hint that much of the reduced upper mantle velocities in northern Tibet[25–27] are located below the Asian LAB. Therefore, the general low velocities in the upper mantle in northern Tibet would not influence the LAB depth. The velocity models in Fig. 3b illustrate the essential differences in the mantle models of southern, central and northern Tibet, which is the lithospheric doubling in the north.

In conclusion, an important observation in the INDEPTH IV data concerning deep lithospheric structure is the identification of a shallow (100–120 km) negative discontinuity in the central and northern Tibetan mantle. We interpret this discontinuity as the Tibetan LAB. The lithosphere in Tibet (crust and mantle part) along the INDEPTH lines shows a surprisingly clear division into three different parts: south of the ZYS we see only the underthrusting Indian lithosphere; north of the KF system we see the Asian lithosphere of the Qaidam basin; in between two LABs indicate a Tibetan lithosphere overriding the Asian lithosphere. It is justified to call this entire region 'Tibetan lithosphere'; although it crosses two suture zones, the Banggong Nujiang Suture and the Jinsha River Suture, it is surprisingly homogeneous.

As the Asian LAB is observed at 140–180 km depth under central–northern Tibet, the Tibetan lithosphere is overriding the Asian lithosphere as India–Eurasia convergence is accommodated in northern Tibet. The observed thin lid of the Tibetan mantle lithosphere could also explain the poor Pn and Sn propagation observed previously in the same region[25–27]. Late arrivals from the 410 and 660 discontinuities also confirm exceptionally slow upper mantle beneath northern Tibet. A similar thin lithospheric mantle lid is also observed below eastern Tibet, but without an Asian LAB beneath. In contrast, the mantle lithosphere in northwestern Tibet, where the LAB occurs at about 220 km depth, is much thicker. This means that the boundary between the lithosphere of the Tibetan plateau and the Asian lithosphere is very different along the three profiles (Fig. 1). Maybe these three structures could be seen as a sequence where first thickening of the Tibetan lithosphere occurs (north-west Tibet), followed by delamination of the lower part of the Tibetan lithosphere (east Tibet) and finally overriding of the Asian lithosphere by the thin Tibetan lithosphere (south of Qaidam basin). However, validity of such a sequence would need confirmation by modelling which is beyond the scope of the present paper.

Received 8 March 2011; accepted 6 October 2011; published online 30 October 2011

References

1. Zhao, J. *et al.* The boundary between the Indian and Asian tectonic plates below Tibet. *Proc. Natl Acad. Sci. USA* **107,** 11229–11233 (2010).
2. Kumar, P., Yuan, X., Kind, R. & Ni, J. Imaging the colliding Indian and Asian lithospheric plates beneath Tibet. *J. Geophys. Res.* **111,** B06308 (2006).

© 2011 Macmillan Publishers Limited. All rights reserved.

3. Kind, R. & Yuan, X. H. Seismic images of the biggest crash on Earth. *Science* **329,** 1479–1480 (2010).
4. Li, C., van der Hilst, R. D., Meltzer, A. S. & Engdahl, E. R. Subduction of the Indian lithosphere beneath the Tibetan Plateau and Burma. *Earth Planet. Sci. Lett.* **274,** 157–168 (2008).
5. Bijwaard, H. & Spakman, W. Non-linear global P-wave tomography by iterated linearized inversion. *Geophys. J. Int.* **141,** 71–82 (2000).
6. Zhang, Z. *et al.* Seismic signature of the collision between the east Tibetan escape flow and the Sichuan Basin. *Earth Planet. Sci. Lett.* **292,** 254–264 (2010).
7. Tapponnier, P. *et al.* Geology–Oblique stepwise rise and growth of the Tibet Plateau. *Science* **294,** 1671–1677 (2001).
8. Zhao, W. & Nelson, K. D. Deep seismic-reflection evidence for continental underthrusting beneath southern Tibet. *Nature* **366,** 557–559 (1993).
9. Brown, L. D. *et al.* Bright spots, structure, and magmatism in southern Tibet from INDEPTH seismic reflection profiling. *Science* **274,** 1688–1690 (1996).
10. Mechie, J., Kind, R. & Saul, J. in *The Seismological Structure of the Tibetan Plateau Crust and Mantle Down to 700 km Depth* 353 (eds Gloaguen, R. & Ratschbacher, L.) 109–125 (Geol. Soc. Lon. Spec. Publ., 2011).
11. Zhao, W. *et al.* Seismology across the northeastern edge of the Tibetan Plateau. *EOS Trans. Am. Geophys. Union* **48,** 487–488 (2008).
12. Yuan, X., Ni, J., Kind, R., Mechie, J. & Sandvol, E. Lithospheric and upper mantle structure of southern Tibet from a seismological passive source experiment. *J. Geophys. Res.* **102,** 27491–27500 (1997).
13. Kosarev, G. *et al.* Seismic evidence for a detached Indian lithospheric mantle beneath Tibet. *Science* **283,** 1306–1309 (1999).
14. Owens, T. J., Randall, G. E., Wu, F. T. & Zeng, R. PASSCAL instrument performance during the Tibetan Plateau passive seismic experiment. *Bull. Seismol. Soc. Am.* **83,** 1959–1970 (1993).
15. Zhu, L. & Helmberger, D. V. Moho offset across the northern margin of the Tibetan Plateau. *Science* **281,** 1170–1172 (1998).
16. Vergne, J. *et al.* Seismic evidence for stepwise thickening of the crust across the NE Tibetan Plateau. *Earth Planet. Sci. Lett.* **203,** 25–33 (2002).
17. Jiang, M. *et al.* Crustal thickening and variations in architecture from the Qaidam basin to the Qang Tang (North-Central Tibetan Plateau) from wide-angle reflection seismology. *Tectonophysics* **412,** 121–149 (2006).
18. Karplus, M. S. *et al.* Injection of Tibetan crust beneath the south Qaidam Basin: Evidence from INDEPTH IV wide-angle seismic data. *J. Geophys. Res.* **116,** B07301 (2011).
19. Yin, A., Dang, Y., Zhang, M., Chen, X. H. & McRivette, M. W. Cenozoic tectonic evolution of the Qaidam basin and its surrounding regions (Part 3): Structural geology, sedimentation, and regional tectonic reconstruction. *GSA Bull.* **120,** 847–876 (2008).
20. Kind, R. *et al.* Seismic images of crust and upper mantle beneath Tibet: Evidence for Eurasian plate subduction. *Science* **298,** 1219–1221 (2002).
21. Wittlinger, G., Farra, V., Hetenyi, G., Vergne, J. & Nabelek, J. Seismic velocities in Southern Tibet lower crust: A receiver function approach for eclogite detection. *Geophys. J. Int.* **177,** 1037–1049 (2009).
22. Nabelek, J. *et al.* Underplating in the Himalaya–Tibet collision zone revealed by the Hi-CLIMB experiment. *Science* **325,** 1371–1374 (2009).
23. Meyer, B. *et al.* Crustal thickening in Gansu–Qinghai, lithospheric mantle subduction, and oblique, strike-slip controlled growth of the Tibet Plateau. *Geophys. J. Int.* **135,** 1–47 (1998).
24. Yin, Y. & Harrison, T. M. Geologic evolution of the Himalayan–Tibetan orogen. *Annu. Rev. Earth Planet. Sci.* **28,** 211–280 (2000).
25. Barazangi, M. & Ni, J. Velocities and propagation characteristics of Pn and Sn beneath the Himalayan arc and Tibetan Plateau: Possible evidence for underthrusting of Indian continental lithosphere beneath Tibet. *Geology* **10,** 179–185 (1982).
26. McNamara, D. E., Walter, W. R., Owens, T. J. & Ammon, C. J. Upper mantle velocity structure beneath the Tibetan Plateau from Pn travel time tomography. *J. Geophys. Res.* **102,** 493–505 (1997).
27. Hearn, T. M. *et al.* Uppermost mantle velocities beneath China and surrounding regions. *J. Geophys. Res.* **109,** B11301 (2004).

Acknowledgements

We thank the station pool of the GFZ Potsdam (www.gfz-potsdam.de/gipp) and the NERC geophysical equipment pool, Seis-UK node (University of Leicester, www.le.ac.uk/seis-uk) for providing seismic stations and support. This research was funded by the CGS-1212010511809 in China, NSF-EAR-CD-0409939 in the USA and the Deutsche Forschungsgemeinschaft and the GFZ Potsdam in Germany.

Author contributions

W.Z., J.M., R.K., R.M., F.T. and Z.W. planned the field experiment. J.M., Z.W., D.S., H.S., G.X., M.K. and F.T. carried out the field experiment. P.K., J.M., R.K. and M.K. did the data analysis and wrote the manuscript.

Additional information

The authors declare no competing financial interests. Supplementary information accompanies this paper on www.nature.com/naturegeoscience. Reprints and permissions information is available online at http://www.nature.com/reprints. Correspondence and requests for materials should be addressed to R.K.

© 2011 Macmillan Publishers Limited. All rights reserved.